The design of a fully-actuated base for a tendon-driven continuum robot manipulator

S. Bezelev (4570235), N.A. van der Lee (4144600), P.J. Stobbe (4601858), J. Vlaardingerbroek (4614003)
Delft University of Technology - Department Precision and Microsystems Engineering - Group A1

***Abstract*— Continuum manipulators have recently grown in popularity due to their compliancy and remote actuation. Unfortunately, a problematic property of tendon-based continuum manipulators is that they are over-actuated. The aim of this paper is to achieve full actuation for tendon-based continuum manipulators. Using cable-length kinematics, several design strategies have been identified. The most promising strategy relies on cancelling out the non-linear kinematic terms through summing cable lengths, and linearising this sum. This linearisation proves reliable for a large range, introducing only a 2.55% error for a curvature arc angle $\theta = 45°$. The performance prototype was benchmarked against an over-actuated model in positioning the end-effector. The realised system shows great potential, displaying high precision, predictable constant offsets, and outperforming the over-actuated model in accuracy.**

I. Introduction

CONTINUUM MANIPULATORS consist of a deformable core structure, that curves continuously and of which the shape can be actuated. In contrast to traditional rigid link robots, continuum manipulators are well suited to unstructured environments due to their inherent compliancy [1]. Therefore these manipulators are found in many applications, ranging from industrial inspections to medical procedures, where they can navigate complex and constrained spaces [2]–[4]. One class of manipulators is the tendon-driven kind, which uses a straightforward and simple to realise actuation strategy [5]. These manipulators are typically actuated using three or four tendons that cause the manipulator to bend with constant curvature by adjusting their length.

A common property of tendon-based continuum manipulators is that they are over-actuated [6]–[9], meaning they use more motors than the number of degrees of freedom their configuration allows. By definition the system is over-constrained, causing large and unwanted forces in the system if the tension in the tendons is not properly distributed [10], [11]. A fully-actuated manipulator does not suffer these drawbacks and it reduces the amount of motors, which enables significant weight reductions.

Few attempts have been made to achieve full actuation. In a planar configuration, full actuation is easier to achieve, and both serpentine and continuum manipulators have been realised with full actuation in a plane [12], [13]. However, full actuation of spatially moving manipulators is more challenging, and only two attempts have been reported. Suh (2018) designed and built a fully-actuated 2 degree of freedom serpentine manipulator [14]. This actuator is not suited for continuum manipulators, because the actuator mirrors serpentine links, whose kinematics are different from continuum manipulators. Only one attempt to realise full actuation in a continuum manipulator has been reported [15]. Here, two tendons are driven, and one is passively tensioned. Unfortunately this actuator suffers from singularity in certain configurations due to the actuator positioning.

This paper covers the design, implementation and evaluation of a novel, full actuation strategy for tendon-based continuum manipulators with three or more equally spaced tendons and two degrees of freedom. Based on the kinematic model, several design strategies are identified. The most feasible strategy is selected and prototyped to experimentally validate the actuation principle. The prototype consists of a summing mechanism, an error reduction mechanism, and two motors. This research is executed within the context of the Bachelor End Project for Mechanical Engineering at the Delft University of Technology.

II. Materials & Methods

A. Kinematic model

Figure 1 shows a generalised schematic for a tendon-based continuum manipulator. Such a manipulator consists of multiple, independently controlled segments. Every segment consists of multiple sections, separated by tendon guides. The shape of all sections in a segment will be equal, and therefore only the kinematics for a single section will be explored in the following section.

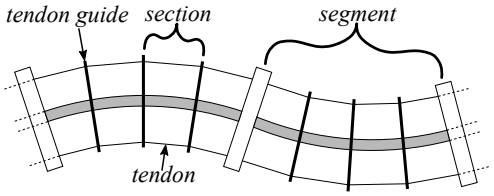

Fig. 1. Generalised multi-segment tendon based continuum manipulator

1) Single section kinematics: Figure 2.a shows the relevant geometric parameters for the manipulator in planar view. The curved line represents the core of the section bending with constant curvature and a constant length of L_0. Vector $\underline{\mathbf{a}}$ is the vector between the start and end position of the section, forming a chord. From its geometry it follows that the length of chord $\underline{\mathbf{a}}$ is:

$$||\underline{\mathbf{a}}|| = 2r\sin(\frac{\theta}{2}), \text{ with } r = \frac{L_0}{\theta} \tag{1}$$

Equation 1 means that the planar position of the manipulator is fully determined by configuration angle θ. In order to bend out of plane, the angle φ needs to be introduced, as seen in figure 2.b. The spatial position of the manipulator is then defined by bending in a plane, and a rotation of that plane around the inertial x-axis. Three holes through which the tendons are routed are also displayed.

2) Cable lengths for a single section: Knowing the position of the end of a section, the required lengths of the tendons in this section can be calculated. As figure 3 shows, a congruent triangle between $\underline{\mathbf{a}}$ and a projection of a tendon on the plane of bending can be constructed, with the tendon parallel to $\underline{\mathbf{a}}$.

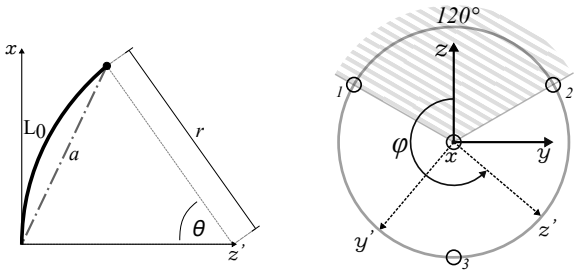

(a) In-plane bending of a single section

(b) Rotation of the bending plane by φ degrees

Fig. 2. Configuration diagrams for a 3-tendon continuum manipulator

The length of any tendon i can be determined by multiplying $||\underline{\mathbf{a}}||$ with the corresponding form factor:

$$l_{c,i} = ||\underline{\mathbf{a}}||(1 + \frac{p}{r}\cos(\varphi + \varphi_{0,i})), \text{ with } r = \frac{L_0}{\theta} \quad (2)$$

$$l_{c,i} = 2\frac{L_0}{\theta}\sin(\frac{\theta}{2}) + 2p\sin(\frac{\theta}{2})\cos(\varphi + \varphi_{0,i}) \quad (3)$$

Here p is the distance between the tendon and the centre line of the core, and $\varphi_{0,i}$ is the angle offset corresponding to cable i. This offset is defined by the angle between the cable base and the z-axis (see 120° in figure 2.b).

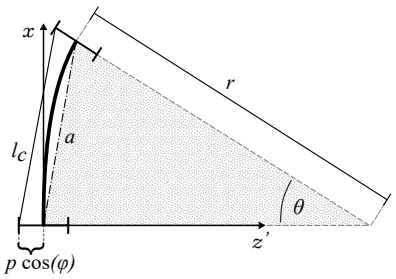

Fig. 3. Congruent triangle relation between chord $\underline{\mathbf{a}}$ and the tendon projection

B. Design

The smallest amount of tendons needed for a spatially moving manipulator is three. This number will be used to explore various design options for full actuation. This means that for a single segment, there will be two actuation inputs and three actuation outputs in total. Two simple ways to achieve this is by either designing a mechanism with two inputs and three outputs, or by designing three parallel mechanisms with two identical inputs and three outputs, one for each tendon.

As can be seen in figure 4, the two-input-one-output mechanisms can implement equations (2) and (3) as either an adding or multiplying mechanism. However, the non-linearities in these equations makes designing such a mechanism difficult. For full actuation the inputs should be θ and φ for each mechanism. Since θ terms are the same for all the tendons, this will not pose a problem. However, since φ is different for each tendon, it is required to have a linear mapping of the motor input to the tendon output for φ, in order to properly drive the mechanisms with a phase difference. The strong non-linearity makes this challenging, if possible at all.

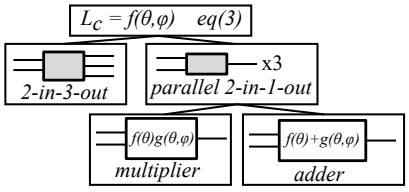

Fig. 4. Design tree of the identified design strategies

From equation (3), it is apparent that the sum of the lengths of any amount of equally spaced tendons is a function only of θ. The φ term cancels out, since 2 or more evenly spaced cosines always sum to zero:

$$L_T = \sum_{i=1}^{n} l_{c,i} = 2n\frac{L_0}{\theta}\sin(\frac{\theta}{2}) \quad (4)$$

By linearisation, this equation further simplifies into:

$$2n\frac{L_0}{\theta}\sin(\frac{\theta}{2}) \simeq nL_0\frac{2}{\theta}\frac{\theta}{2} \simeq nL_0 \quad (5)$$

The error in length due to linearisation increases slowly with respect to θ, due to the two fractions in equation 4. When bent up to $\theta = 45°$, the error $\epsilon = |1 - \frac{2}{\theta}\sin(\frac{\theta}{2})|$ will be 2.55%. Therefore the total cable length can initially be assumed constant, meaning the sum of the displacements of all cables must be zero. Hence for a 3-tendon continuum manipulator, a subsystem could be designed that takes the displacement of two tendons as input, and outputs the displacement of the third tendon:

$$\Delta l_{c,3} = -(\Delta l_{c,1} + \Delta l_{c,2}) \quad (6)$$

This allows for the actuator to be decoupled into two serial subsystems: one that sums the cable displacements to zero, and a second one altering the total length to ensure equation (4) is realised, compensating for the error introduced in equation (5). Then, two cables can be controlled directly using equation (3), with the length of the third cable determined by the summing mechanism. This approach of a summing subsystem and an error negating subsystem, as shown in figure 5, works for any amount of equally spaced tendons, as the linearisation process holds for any amount of tendons.

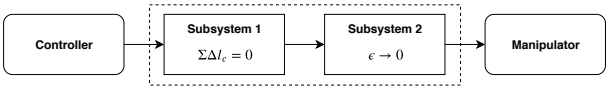

Fig. 5. Design options for transmission mechanisms

C. Prototype design

The summing mechanism that implements equation (6) is realised with a planetary gearbox as seen in figure 6. The three tendons are each connected to a pulley. Two pulleys, red and green, are each connected to a stepper motor that directly controls the length of the connected tendons. The third, yellow, pulley is connected to both stepper motors via the planetary gearbox. This planetary gearbox uses the red ring gear and green carrier as inputs, and the yellow sun gear as output, making the rotation of the sun the sum of the rotation of the other pulleys as in equation (6).

This entire mechanism is modular and can be swapped out for an over-actuated base for comparing experimental results.

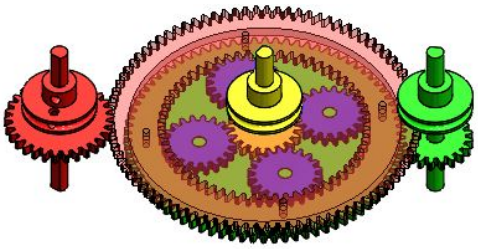

Fig. 6. Gearbox that functions as the adding mechanism

Since the error in total cable length is small compared to the intended total cable length, the slack due to the error can be reduced by a cable tensioner.

The manipulator consists of a central rod that is considered of constant length, and five discs that guide the tendons along the rod towards the end-effector, dividing the manipulator into six sections. It is actuated by three tendons, which are spaced equally around the central rod. The manipulator core is a PEEK rod, with a length of 285mm and diameter of 6mm. The distance between the core centre-line and the cable centre-line p is 21.5mm, based on a maximum θ of $45°$ so that the tendons will not intersect with the rod.

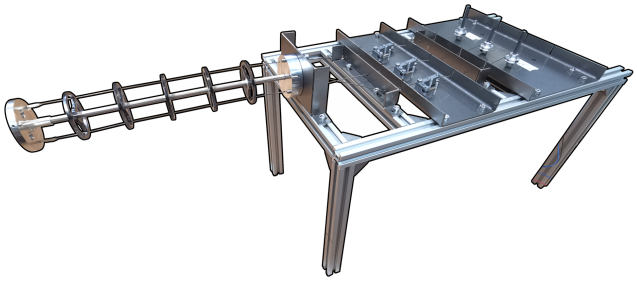

Fig. 7. The assembled prototype

D. Experimental work

1) Prototype operation: The experimental setup consists of a DC power source connected to an Arduino with a stepper motor shield. The Arduino is connected to a computer within a ROS framework. Python nodes in this ROS framework process positioning requests, calculate the desired motor positions, and send these positions to the Arduino. The position of the end-effector is then photographed frontally from a distance of 3m with a high zoom. This ensures near orthographic projection. This reduces image warping effects due to perspective.

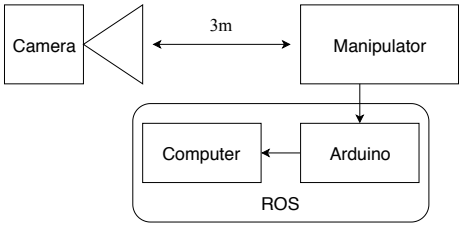

Fig. 8. Diagram of the experimental setup

2) Experimental validation: The performance in positioning the end-effector of the fully-actuated manipulator with feed forward control is compared to the positioning by an identically controlled over-actuated manipulator. This test is conducted for θ of $5°$, $10°$ and $15°$, and φ ranging from $0°$ to $180°$, with increments of $30°$. The tests are conducted in five consecutive runs per θ. The resulting images are then analysed using the open source software ImageJ [16], resulting in z and y position data that is processed in MS Excel and MATLAB.

The intended position is defined as $\underline{\mathbf{p_I}}$, and the fully-actuated position is defined as $\underline{\mathbf{p_{FA}}}$. Using these positions, two errors can be defined:

- A normalized error in deflection: $\epsilon_\rho = \frac{||\underline{\mathbf{p_{FA}}} - \underline{\mathbf{p_I}}||}{||\underline{\mathbf{p_I}}||}$.
- An error in rotation of the bending plane, φ: $\epsilon_\varphi = \angle(\underline{\mathbf{p_{FA}}}, \underline{\mathbf{p_I}}) = \texttt{atan2}(||\underline{\mathbf{p_I}} \times \underline{\mathbf{p_{FA}}}||, \underline{\mathbf{p_I}} \cdot \underline{\mathbf{p_{FA}}})$, where $\texttt{atan2}(\cdot,\cdot)$ is the four-quadrant inverse tangent.

III. Results

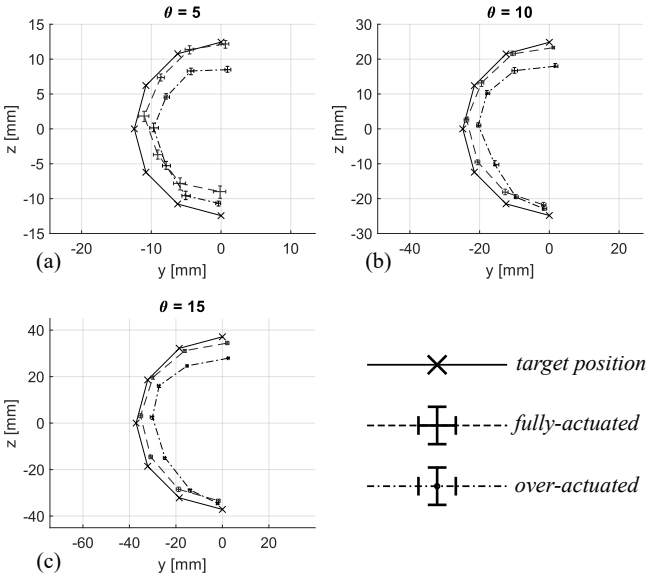

Fig. 9. Positioning test results of the fully-actuated and over-actuated model, along with the intended position

Figure 9 shows the results of the positioning tests of both the fully- and over-actuated models, along with the intended position. Both have a precision with the standard deviation below 1mm. The fully-actuated model displays better accuracy, with results getting closer to the intended position as θ increases.

Focusing on the fully-actuated manipulator, figure 10 shows the positioning errors in polar coordinates. As seen in figure 10.a, the normalised error ϵ_ρ increases as φ moves towards $180°$. The error in φ is displayed in figure 10.b and is largest near $\varphi = 90°$.

IV. Discussion

The over-actuated model displays a repeating error in positioning. Similar errors for open loop over-actuated manipulators have - without further elaboration - been reported by other researchers [7], [9]. In our tests, the error is likely caused by insufficient tension in the tendons when the manipulator is at rest.

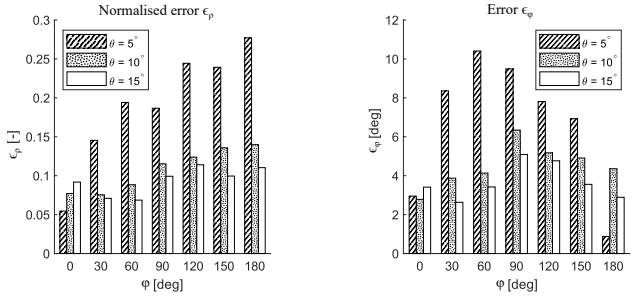

(a) The positioning error (ϵ_ρ), normalised over the radius of the intended position

(b) The error in φ, not normalised

Fig. 10. Polar positioning errors of the fully-actuated manipulator with respect to the intended position

The errors in positioning the fully-actuated manipulator are caused by the control scheme. The tendons directly linked to the motors are always rotated such that the length is exactly known, thus the error in cable length only manifests in the third tendon. This error should be compensated by the tensioners. However, as φ approaches $180°$, the third tendon moves to the inside of the curvature and the required tension on this tendon becomes too much for the spring in the tensioner to handle. The tensioner will hit its end stop, leaving the error in the third cable.

This results in two errors. The first is a smaller curvature ($\kappa = \theta \backslash L_0$), since a tendon on the inside of the curvature is too long and the core rod exerts a force to return to its unbent shape. This effect will be greatest with φ between $150°$ and $210°$, when the third tendon is the only tendon on the inside of the curvature. The second error is in φ. When two tendons are on the inside of the curvature, and one of those is too long, φ will be pulled towards the shorter tendon. In this case the error is observed for φ between $30°$ and $150°$, as in this region both the directly actuated first tendon and the indirectly third tendon are located on the inside of the curvature. These errors can be reduced by improving the control scheme, thereby moving the error to the outer tendons. Alternatively, the cable tensioners can be replaced with a mechanism that better enforces error reduction.

V. Conclusion

This paper presents a novel and easily implementable strategy for full actuation of tendon-based continuum manipulators, which is feasible both theoretically and practically.

The kinematic model was used to set up various design strategies. The most promising strategy relies on cancelling out the multi-variable non-linear kinematic terms through summing cable lengths, and linearising this sum. This linearisation proves reliable for a large range, introducing only a 2.55% error for a curvature arc angle $\theta = 45°$. A prototype using this strategy was designed, realised, and compared with the over-actuated strategy using a modular construction. The realised system shows great potential, displaying high precision, predictable constant offsets, and outperforming the over-actuated model in accuracy. These offsets are due to the error distribution over the tendons.

Further research should aim to improve the current design and explore new possibilities. Improving the control scheme will reduce the positioning errors. Also, new mechanical solutions for the error reduction mechanism should be identified. These solutions should actively enforce the cable lengths instead of passively compensating. Further exploration and identification of design strategies is needed. Finally, the system could be extended to a multi-segment manipulator.

Ultimately, this will lead to more reliable and lighter continuum manipulators. These improvements are a significant step for industrial inspections, medical procedures, and work in unstructured and constrained environments.

Acknowledgements

We would like to thank Andres Hunt and Hassan Hossein-Nia for their guidance, Jelle Mens, Simon van der Marel and Jeroen Gijzemijter for their instructions and assistance in manufacturing, Bradley But for the technical support, and Blozo and BUDI for sponsoring parts.

References

[1] G. Robinson and J. Davies, "Continuum robots - a state of the art," *Proceedings 1999 IEEE International Conference on Robotics and Automation (Cat. No.99CH36288C)*, 1999.

[2] H. B. Gilbert, J. Neimat, and R. J. Webster, "Concentric tube robots as steerable needles: Achieving follow-the-leader deployment," *IEEE Transactions on Robotics*, vol. 31, no. 2, 2015.

[3] "Robotic solutions for confined and hazardous environments." [Online]. Available: http://www.ocrobotics.com/

[4] A. Wolf, H. Brown, R. Casciola, A. Costa, M. Schwerin, E. Shamas, and H. Choset, "A mobile hyper redundant mechanism for search and rescue tasks," *Proceedings 2003 IEEE/RSJ International Conference on Intelligent Robots and Systems (IROS 2003)*, 2013.

[5] I. D. Walker, "Continuous backbone continuum robot manipulators," *ISRN Robotics*, 2013.

[6] J. Back, L. Lindenroth, K. Rhode, and H. Liu, "Three dimensional force estimation for steerable catheters through bi-point tracking," *Sensors and Actuators A: Physical*, vol. 279, Jun 2018.

[7] L. Minhan, R. Kang, S. Geng, and E. Guglielmino, "Design and control of a tendon-driven continuum robot," *Transactions of the Institute of Measurement and Control*, vol. 40, 2018.

[8] J. Back, R. Karim, Y. Noh, K. Rhode, K. Althoefer, and H. Liu, "Tension sensing for a linear actuated catheter robot," *Intelligent Robotics and Applications Lecture Notes in Computer Science*, 2015.

[9] R. J. Roesthuis, S. Janssen, and S. Misra, "On using an array of fiber bragg grating sensors for closed-loop control of flexible minimally invasive surgical instruments," *2013 IEEE/RSJ International Conference on Intelligent Robots and Systems*, 2013.

[10] D. Camarillo, C. Milne, C. Carlson, M. Zinn, and J. Salisbury, "Mechanics modeling of tendon-driven continuum manipulators," *IEEE Transactions on Robotics*, vol. 24, no. 6, 2008.

[11] D. Camarillo, C. Carlson, and J. Salisbury, "Configuration tracking for continuum manipulators with coupled tendon drive," *IEEE Transactions on Robotics*, vol. 25, no. 4, 2009.

[12] J.-W. Suh and K.-Y. Kim, "Harmonious cable actuation mechanism for soft robot joints using a pair of noncircular pulleys," *Journal of Mechanisms and Robotics*, vol. 10, no. 6, Aug 2018.

[13] I. Gravagne, C. Rahn, and I. Walker, "Large deflection dynamics and control for planar continuum robots," *IEEE/ASME Transactions on Mechatronics*, vol. 8, no. 2, 2003.

[14] J.-W. Suh, "A novel cable actuation mechanism for 2-dof hyper-redundant bending robot composed of pulleyless rolling joints," *2018 IEEE/RSJ International Conference on Intelligent Robots and Systems (IROS)*, 2018.

[15] P. A. E. Francis, "Design and modelling of a miniature instrument for robotic surgery," 2017.

[16] W. Rasband, "Imagej." [Online]. Available: https://imagej.nih.gov/ij/?